Comparative study using spheres, rods and spindle-shaped nanoplatelets on dispersion stability, dissolution and toxicity of CuO nanomaterials

Misra, Superb K; Nuseibeh, Samir; Dybowska, Agnieszka; Berhanu, Deborah; Tetley, Teresa D; Valsami-Jones, Eugenia

DOI:
10.3109/17435390.2013.796017

The effect of nanoparticle morphology on dispersion stability, dissolution and toxicity: Comparative study using copper oxide spheres, rods, and spindle shaped nanoplatelets

Superb K. Misra[1,2‡], *Samir Nuseibeh*[3‡], *Agnieszka Dybowska*[2], *Deborah Berhanu*[2], *Teresa D.Tetley*[3], *Eugenia Valsami-Jones*[1,2]

[1]School of Geography, Earth & Env. Sciences, University of Birmingham, B15 2TT, UK

[2]Dept. of Earth Sciences, Natural History Museum, Cromwell Road, London SW7 5BD, UK

[3]Lung Cell Biology, National Heart & Lung Institute, Imperial College London, London, UK

* Corresponding author: s.misra@bham.ac.uk ; s.misra@nhm.ac.uk

‡These authors contributed equally.

ABSTRACT

Copper oxide nanoparticles with different shapes were used to examine the effect of shape on the various physicochemical properties (reactivity, aggregation, suspension stability) and to examine the behaviour by which CuO nanoparticles exhibit their biological response towards alveolar type-I cells. The different shapes examined in this study include spherical, rod and spindle shaped platelet particles. *In vitro* dissolution studies (7 days) in 1mM $NaNO_3$ matrix showed a marked difference in dissolved Cu release between the nanoparticles. However, in serum-free cell culture media (exposure media to cells) the particles' dissolution was found to be significantly enhanced with close to complete dissolution reported for all particle types. Biological studies showed both shape and size of the CuO nanoparticles tested to have a significant effect on TT-1 cell viability and release of pro-inflammatory cytokines; IL-6 and IL-8. This study shows a complex interplay between particulate and dissolved species triggering the biological response. Upon immediate exposure of CuO nanoparticles of different shapes, the particulate form contributes towards the toxicity. However, for any biological response observed over and beyond a period of 24 hrs the dissolved fraction becomes significant.

KEYWORDS: Nanoparticles; Copper oxide; Dissolution; Shapes; Nanotoxicology

1. INTRODUCTION

The interaction of particles with cells is shown to be strongly influenced by particle size. However, emerging studies have started to highlight that size may not be the only critical factor that governs the biological response of nanoparticles, with surface chemistry (Liu et al. 2010), shape (Gratton et al. 2008; Huang et al. 2010, Stoehr et al. 2011) and particle solubility (Studer et al. 2010; Franklin et al. 2007) all having the potential to play a pivotal role. Therefore, isolating the parameters that affect biological response often becomes difficult due to the lack of particles where different variables (size, shape, surface area, and surface chemistry) can be independently altered one at a time. Often to validate this, nanoparticles of different compositions are tested in different studies and the results joined together to answer "physicochemical properties dependent toxicity". This approach hinges on the assumption that all the physicochemical properties affect the nanoparticles of different composition equally, which often may not be the case. For example, size may play an important role in triggering a biological response for silica nanoparticles (Yu et al. 2009) but for zinc oxide nanoparticles it may be their rate of dissolution (Franklin et al. 2007) which determines their biological response while for Ag nanoparticles both the effect of particle size and dissolution have been shown as contributing factors (Liu et al. 2010; Kim et al. 2012).

Synthesizing nanoparticles of different shapes is at present intensely exploited due to the enhanced shape specific properties at the nanoscale. Optical, mechanical and electrical properties of nanomaterials have been shown to be affected by the shape of the nanocrystals. Apart from the material and physicochemical properties, shape also seems to have an effect on the biological response (Venkataraman et al. 2011)

and even on the antimicrobial effect (Pal et al. 2007) of the nanoparticles. Studies using polymeric nanoparticles (Venkataraman et al. 2011) have shown that shape of the particles can have an effect on their bio-distribution, internalization (phagocytosis and endocytosis), and cytotoxicity. Various articles (Gratton et al. 2008; Huang et al. 2010; Venkataraman et al. 2011; Stoehr et al. 2011) have suggested shape of the nanoparticles to play a profound role on the biological response. For example, long rod silica particles (450x110 nm) were taken up in larger amounts, with faster internalization by A375 human melanoma cells than spherical (100 nm) and short rod (240x120 nm) silica nanoparticles (Huang et al. 2010). Similarly long rod silica particles had a greater impact on cell proliferation, apoptosis, cytoskeleton formation, adhesion and migration. Pal et al. (2007) demonstrated shape to play a key role in the antimicrobial property of silver nanoparticles, wherein truncated triangular nanoplates (with {111} plane as the basal plane) having a stronger biocidal action than spherical and rod-shaped nanoparticles. For silver, wire shaped particles have shown to significantly reduce cell viability and increase LDH release for A549 cells, whereas no effect on the alveolar epithelial cells was observed for spherical silver particles (Stoehr et al. 2011).

Often, the mode by which the nanoparticles exhibit toxic response varies from particulate derived (Yu et al. 2009), dissolution based (Franklin et al. 2007), oxidative stress related (Li et al. 2012) to Trojan horse based mechanism (Park et al. 2010). The preferred route varies for each particle type (including their physicochemical properties) and often can be a combination of the above mechanisms. For example, titanium dioxide and zinc oxide nanoparticles have a high propensity to generate reactive oxygen species (Li et al. 2012), silver nanoparticles have been shown to

exhibit Trojan horse mechanism based toxicity (Park et al. 2010; Navarro et al. 2008) and solubility of zinc oxide nanoparticles has contributed to dissolution based toxicity (Franklin et al. 2007).

Copper oxide nanoparticles are used for various applications (viz. catalysts, microelectronics, solar energy, high temperature superconductivity), with also several reports on their enhanced bactericidal effect (Baek et al. 2011). Limited biological studies on CuO nanoparticles have shown them to induce significantly higher toxicity in mammalian cell lines (Karlsson et al. 2009; Ahamed et al. 2010) compared to bulk CuO particles. Instead of a single predominant mode of biological response a likely combination of dissolved species generated from the nanoparticles (Studer et al. 2010) and ROS (reactive oxygen species) mediated oxidative stress (Gunawan et al. 2011) are thought to be the primary mechanism of CuO nanoparticles toxicity. Although most of the biological studies performed on CuO nanoparticles are based on bulk vs. nanosize comparison, little if anything is known about the effect of particle shape on CuO toxicity. Therefore, in this study three different shapes (spheres, rods and spindles) of CuO nanoparticles were synthesized to examine the effect of shape on (a) the physicochemical properties of CuO nanoparticles, (b) dissolution and stability of these nanoparticles in 1mM $NaNO_3$ medium and DCCM-1 cell culture medium, (c) the biological response of these nanoparticles on human, alveolar type-1 epithelial cells (TT-1 cells). Finally, this study also addresses comparatively whether the observed biological response from TT-1 cell lines is a particulate or dissolution derived effect.

2. MATERIALS & METHODS

2.1 *Particle synthesis:* CuO nanoparticles of three different shapes i.e. sphere, rods and spindles were prepared using wet chemistry and $CuCl_2.2H_2O$ as the precursor (Zhu et al. 2004, Misra et al. 2012;). For spherical CuO (CuO-s) nanoparticles, 0.02 M of $CuCl_2.2H_2O$ was dissolved in 150 mL deionised water and 500 μL of glacial acetic acid was added to the solution. The solution was then heated to 100°C followed by a rapid addition of 0.65 g NaOH. For rod shaped CuO (CuO-r) nanoparticles, 0.02 M of $CuCl_2.2H_2O$ was dissolved in 150 mL deionised water and heated to 100°C followed by a rapid addition of 0.8 g NaOH. Similarly, for spindles (CuO-spindles) 0.02 M of $CuCl_2.2H_2O$ was dissolved in 150 mL deionised water with addition of 500 μL of glacial acetic acid and 0.8 g NaOH. The solution was then heated to 100°C and kept at that temperature for 5 mins, before cooling it to room temperature. The resulting black precipitate for all samples was centrifuged and the nanoparticles were repeatedly washed (3 times) with de-ionized water to get phase pure CuO nanoparticles, prior to further characterisation as described below. All the three types of CuO NPs were easily re-suspended in deionised water forming stock suspension from where appropriate dilutions were made for biological testing.

2.2 *Particle characterization:* Diluted suspension of the nanoparticles was deposited on copper grid for TEM imaging (Hitachi 7100, 100 kV). X-ray diffraction was performed on the nanoparticles using Enraf-Nonius diffractometer coupled to INEL CPS 120 position-sensitive detector with Co-K_α radiation and the phase identification was performed using STOE software. BET analysis (Micromeritics) was performed on the dried CuO nanoparticles after washing. For AFM measurements,

diluted CuO suspensions was deposited onto freshly cleaved mica substrate attached on a glass slide and allowed to air dry in a clean environment. AFM was conducted on the samples, using Asylum MFP-3D-SA (Santa Barbara, USA) instrument in AC mode. The samples were scanned in air using an Olympus AC-240TS tip (spring constant 2 N/m). The hydrodynamic size and zeta potential of the nanoparticles were measured using Malvern Zetasizer (Malvern Instruments). ICP-AES (Varian Instruments) analysis was performed to determine the initial concentration of CuO in the aqueous nanoparticulate suspension and also measure the dissolution of the nanoparticles as described below.

2.3 *Particle reactivity and dissolution studies:* Reactivity studies on CuO nanoparticles were performed at a Cu concentration of 750 mg/L by using zeta potential and hydrodynamic size measurements. The effect of temperature on zeta potential and hydrodynamic size of CuO nanoparticles was measured in water using a Malvern Zetasizer (Malvern Instruments). The effect of pH on the zeta potential was measured in water to assess the colloidal stability of all the particle types. The stability of the CuO particle suspension in cell culture media was also investigated using Malvern Zetasizer. Particle dissolution was measured using dialysis membranes (Misra et al. 2012) and centrifugal ultrafiltration (Navarro et al. 2008; Liu and Hurt, 2010). All samples were thoroughly washed before the dissolution experiment and appropriate blanks were included in the experimental set up to control for a potential contamination from reagents and containers. 10 mL of CuO particulate suspension (in water) was placed inside a dialysis bag (MWCO=12.4 kDa) and transferred to 250 mL plastic bottles (Nalgene) containing 200 mL of 1 mM $NaNO_3$

(pH=6.7). The starting Cu concentration inside the dialysis bag for all the dissolution experiments was kept constant at 750 mg/L, with the exception of a series of experiments conducted on CuO-spindles, where the initial concentration varied from 5 to 50 mg/L. Soluble Cu nitrate salt was used as the source of ionic Cu. The bottles were incubated at 25°C and 200 rpm (Stuart Scientific Instruments shaker incubator). Aliquots of 1 mL were taken from the media outside the dialysis bag at regular interval, acidified with 5% HNO_3 and the concentration of Cu was then measured using ICP-AES (Varian Instruments). At the end of the dissolution experiment, aliquots of the suspensions inside the dialysis bag were examined by TEM to ascertain the presence of nanoparticles.

Dissolution experiments were also performed in DCCM-1 cell culture media using centrifugal ultrafiltration to minimise the excessive use of cell culture media. The results obtained from both the techniques (i.e. Dialysis membrane and Centrifugal filtration units) were highly comparable as demonstrated in our control experiments (Supporting Information S2). The study was conducted on all the three types of particles (at a concentration of 51, 48 and 61 mg/L) suspended in 50 mL of DCCM-1 media and incubated for 24 hrs at 37 °C under static conditions. At regular time points , 2 mL of the particle suspension in the media was withdrawn and transferred into 15 mL centrifugal filtration units (Millipore, 3 kDa) containing 8 mL of deionised water, which was then centrifuged at 6000g for 30 mins (Eppendorf Centrifuge, 5810). The use of the centrifugal filter units ensured the separation of nanoparticles from the suspension. The filtrate part was then digested using 5% HNO_3 before ICP-AES analysis.

2.4 *Cell Culture:* To evaluate the toxicity and bioreactivity of CuO-r, CuO-s and CuO-spindles, the TT-1 cell line was used. The TT-1 cell line was established in-house by transforming alveolar type-2 cells, isolated from human lung tissue, by lentiviral transduction (ref: PMID: 18539954). TT-1 cells have an alveolar type-1 cell phenotype and morphology (ref: PMID: 18539954). TT-1 cells were cultured as previously described (ref: PMID: 18539954), in humidified 5% CO_2 air and at 37°C. Cells were cultured in DCCM-1 media (Biological Industries, Israel) supplemented with 10% New Born Calf serum (NCS; Invitrogen, Paisley, UK) and 1% penicillin/streptomycin/glutamine (PSG; Invitrogen). For nanoparticle exposures, cells were passaged and seeded into 96-well plates (Greiner Bio One, Stonehouse, UK), then grown until 80% confluent. Once cells had reached 80% confluency, the culture media was removed and replaced with serum-free media and cultured for a further 24 hrs, prior to particle exposure. For particle exposure, a stock suspension of 1mg/mL was prepared in deionised water by direct dilution of the synthesised CuO nanoparticles aqueous suspension. No further surfactants/dispersant were added to ensure dispersion of the particles at the concentrations required for the biological tests, as the particles were suspending easily using vortex in the serum free DCCM-1 media .

2.4.1 *MTT Assay:* Following the 24 hrs exposure period to the nanoparticles, the cell culture exposure media was removed and cells were washed 3 times in warm PBS (to remove any residual nanoparticles). After washing, cells were then incubated for 1h and at 37°C in serum-free media containing 0.5 mg/mL 3-(4,5-Dimethylthiazol-2-yl)-2,5-diphenyltetrazolium bromide (MTT–Sigma Aldrich, UK). MTT-containing media was then removed and 200 µL DMSO (Sigma Aldrich, UK) was added to each

well to lyse the cells and dissolve the insoluble formazan crystals. Prior to the measurement of optical densities, the 200 µL DMSO solution from each well was transferred to a v-bottom, 96 well plate (Greiner Bio One, Stonehouse, UK) and centrifuged at 14,000 g for 20 min to remove any residual nanoparticles. Optical densities were measured using a Thermomax 2 microplate reader at 550 nm (MTX Lab Systems, USA) and cell viability was calculated as a percentage of unexposed, control cells. To determine the effect of nanoparticles on the MTT assay, nanoparticles were: (i) added to unexposed, control cells immediately before the assay, or (ii) added to the assay system following DMSO dissolution and then processed identically to cellular experimental cells.

2.4.2 Cytokine release: The concentrations of IL-6 and IL-8 released by TT-1 cells during exposure to CuO-s, CuO-r, and CuO-spindles were analysed by ELISA. After exposure to nanoparticles, cell culture media supernatants were transferred to a v-bottom, 96-well plate and centrifuged at 14,000 g for 20 min to remove any residual nanoparticles. Supernatants from this centrifugal process where then taken and analysed for cytokine release, using commercially available, quantitative sandwich ELISA kits (DuoSet ELISA kits; R&D systems, Abigndon, UK) according to the manufacturer's recommendations. All measurements were performed in triplicate.

2.4.3 Reactive oxygen species (ROS) study: Generation of reactive oxygen species after exposure to CuO nanoparticles was measured using the fluorescent, free-radical sensor, dihydroethidium (DHE – Invitrogen, Paisley, UK). Cells were serum starved for 24 hrs prior to exposure to particles for 4 hours. After exposure, cells were washed twice in warm, serum-free media then incubated for 25 mins at 37°C and 5% CO_2 in serum-free media containing 40 µM DHE. The DHE probe was then

removed and cells were again washed twice in warm, serum free media to remove any residual DHE. Fluorescent microscopy and image capture software (SimplePCI software, Digital Pixel, UK) was used to analyse ROS generation.

3. RESULTS

3.1 Size, surface area and morphology

Three different shapes of CuO nanoparticles synthesized in this study were characterized using a range of analytical techniques. The size, shape and crystal phase of the synthesized nanoparticles are shown in Fig. 1-3. In Fig. 1, TEM images of spherical, rod shaped, and spindle shaped nanoplatelets of CuO-spindles are shown. The synthesized CuO-s nanoparticles had a size of 7±1 nm with a narrow size distribution and were found to be in a non-aggregated state. In the case of nanorods, the nanoparticles were 7±1 nm in width and 40±10 nm in length. Compared with the spheres, there was more polydispersity in the length of the rods and less so in their diameter, also the nanoparticles were more agglomerated, as shown in Fig. 1b. For spindles the longitudinal length was 1.14±0.24 μm and axial width was 270±50 nm (Fig. 1c). Fig. 2 shows the AFM analysis performed on the synthesized nanoparticles. The spherical nature of the CuO-s nanoparticles was confirmed through AFM imaging, as the height of the nanoparticles was measured to be of 8±1 nm. For CuO-r nanoparticles, the height of the individual nanorods was 9±1 nm. However, for CuO-spindles sample the height of the nanoparticles was measured to be 30±10 nm. The dimension of the CuO-spindles taken in conjunction with the TEM and AFM measurements denotes the particles to be of plate like morphology with a 2D-shape of spindles (Fig. 2d). All three shaped particles have at

least one of their dimensions below the 100 nm range, as shown by all the analysis (all 3 dimensions for CuO-s, 2 dimensions and CuO-r, and 1 dimension for CuO-spindles particles). Another measure of size is hydrodynamic diameter, which refers to how a particle diffuses within a given fluid. The hydrodynamic size of CuO-s nanoparticles measured in water was 76 nm and 150 nm in cell culture medium (DCCM-1). The DLS technique employed in this study to measure hydrodynamic size of the nanoparticles is not accurate for non-spherical nanoparticles and hence only the DLS size of the CuO-s nanoparticles is quoted. The crystal phase identified by XRD for all the nanoparticles was to be of tenorite (ICDD 48-1548), as shown in Fig. 3. The measured Brunauer-Emmett-Teller (BET) surface area for CuO-s, CuO-r and CuO-spindles were 60, 51 and 18 m^2/g, respectively (Table 1). This large difference in specific surface area for the samples stems from the differences in the size and shape of the nanoparticles.

3.2 Stability of CuO nanoparticles

The stability of the nanoparticles suspension in deionised water and in cell culture media was assessed using zeta potential (ξ) measurements. All the samples were positively charged with a ξ value of 48, 43 and 36 mV in deionised water for CuO-s, CuO-r and CuO-spindles, respectively. The relative high ξ values indicate the stability of the nanoparticles in deionised water. The effect of temperature on the stability of the aqueous nanoparticles suspension was measured by monitoring the change in ξ of the samples over a temperature range of 15-50°C. There was a considerable decrease in ξ with increase in the temperature for all the CuO nanoparticles (12% for CuO-s, 16% for CuO-spindles and 24% for CuO-r), as shown in Fig. 4A. Additionally,

the effect of pH on the stability of CuO nanoparticles (Fig. 4b) in 1 mM $NaNO_3$ at 22 °C was also measured. Stability of the suspension decreased with increasing the pH as samples were approaching the point of zero charge (PZC), which for CuO-s nanoparticles was found around pH 9.87, for CuO-r nanoparticles around pH 9.13 and for CuO-spindles around pH 8.34. In contrast to the high ξ of the nanoparticles in water, when suspended in cell culture media, the ξ of the nanoparticles reduced considerably at room temperature (Table 1). This difference in zeta potential has been well documented by Lundqvist et al (2008) to occur due to the interaction of the nanoparticle surface with the molecular components of the cell culture medium.

3.3 Copper release

The dissolution of CuO nanoparticles was measured in 1 mM $NaNO_3$ (pH=6.7) solution using dialysis membranes (Misra et al. 2012) for a period of up to 7 days. The use of dialysis membrane and centrifugal ultrafiltration for the experiments ensured that only the dissolved fraction of copper contributes to the measurement and not the nanoparticles. Fig. 5 shows the dissolved copper (Cu^{2+}) fraction released from the nanoparticles. The equilibrium concentration of dissolved copper was found to be significantly different between three types of nanoparticles. Dissolved copper of up to 1, 0.4 and 0.31 mg/L was released from CuO-s, CuO-r, and CuO-spindles, respectively. The corresponding wt. % of nanoparticles dissolved from the samples was 2.5%, 1.1% and 0.8% for CuO-s, CuO-r and CuO-spindles, respectively (Fig. 5b). Diffusion of dissolved Cu through the dialysis membrane was fast, with up to 95% Cu recovery within the first few hours, as shown in the case of the soluble copper nitrate that was used as the ionic control. TEM analysis of the nanoparticles

suspensions from inside the dialysis bag after the dissolution experiments confirmed the presence of nanoparticles (data not shown). The dissolution data obtained for the samples were described by first-order Noyes-Witney equation (Costa et al. 2001).

$$y(t) = y_{final}(1 - \exp^{-kt}) \quad (1)$$

With *y(t)* the released amount of copper (ppm), y_{final} the final steady state concentration of the released copper, *k* the rate coefficient, and *t* the time in hours. The values for y_{final} and *k* were extracted from the data (selected through least square fitting). The rate coefficient of dissolution curve for the samples followed the order of k_{CuO-s} (0.32 h^{-1})> k_{CuO-r} (0.050 h^{-1})> k_{CuO-sp} (0.022), which further highlights the difference in dissolution kinetics between the three different shaped nanoparticles. The release of dissolved Cu was fastest from the ionic source, followed by CuO-s nanoparticles and slowest for the CuO-spindles. To examine the effect of starting concentration on the dissolution of CuO nanoparticles, a range of starting concentration of CuO-spindles (5-50 mg/L) were used. The results (Fig. 5c-d) demonstrated a significant increase in the apparent dissolved Cu concentration with time on increasing the starting concentration. However, when normalised by mass, there was a significant decrease in % dissolution of CuO-spindles with increasing starting concentration. A similar concentration dependent dissolution has also been reported for various other types of nanoparticles (Misra et al. 2012; Liu and Hurt, 2010).

Within this study, the dissolution of CuO nanoparticles was also measured in serum free DCCM-1 media to facilitate a better understanding of the nanoparticles

biological response. Under static conditions the spheres and rods showed a high degree of dissolution over time (Table 2), with close to 81% dissolution within 4 hrs and staying constant for a period of 24 hrs. However, for spindles there was a gradual increase in dissolution with time. The % dissolution for CuO-spindles increased from 40% to 64% by the end of 24 hrs. In addition, the marked differences in the release of dissolved Cu between the samples, as observed in 1mM $NaNO_3$ medium, was no longer so evident in the DCCM-1 medium.

3.4 Particle toxicity

Particle toxicity was assessed using MTT assay, cytokine release study and oxidative stress measurements. TT-1 cell viability greatly reduced after 24 hrs exposure to both CuO-r and CuO-s nanoparticles (Fig. 6). Whilst concentrations of 0.1 and 1 μg/mL were tolerated, 5, 10, 25 and 50 μg/mL caused a statistically significant, concentration-dependent decrease in cell viability, ranging from 75 – 90% loss (compared with non-treated controls, Fig. 6). In contrast to these effects, exposure to the CuO-spindles did not significantly alter TT-1 cell viability (Fig. 6). TT-1 cell release of the two pro-inflammatory cytokines; IL-6, and IL-8 were measured after 24 hr exposure to the three CuO nanoparticles by ELISA. IL-6 release was significantly elevated above baseline after 24 hrs exposure to both 1 μg/mL CuO-r and 1 μg/mL CuO-s, by approximately 7- and 5-fold respectively (Fig. 7a). However, this was the maximal level of release observed for both nanoparticles since IL-6 concentrations then concentration-dependently decreased back down to baseline, as particle concentration increased (Fig. 7a). In the case of exposure to the CuO-s nanoparticles, IL-6 concentrations went from being significantly elevated above baseline controls at

1 μg/mL, to being significantly lower than baseline controls at 50 μg/mL (Fig. 7a). In stark contrast to both the CuO-r and CuO-s nanoparticles, exposure to the CuO-spindles resulted in a concentration-dependent increase in IL-6 release, becoming statistically elevated above baseline controls at a concentration of 10 μg/mL (Fig. 7a). IL-6 release reached a maximal, 12-fold increase above non-treated, baseline secretions at the highest concentration of CuO-spindles tested – 50 μg/mL. Although CuO-r and CuO-s nanoparticles induced elevated levels of IL-8 at concentrations of 1, 5 and 10 μg/mL, none of these observations were statically significant (Fig. 7b). However, exposing TT-1 cells to higher concentrations (25 and 50 μg/mL) of both CuO-r and CuO-s nanoparticles resulted in significant inhibition of IL-8, below that of baseline secretions (Fig. 7b). Exposure to the CuO-spindles resulted in no significant changes at all concentrations tested (Fig. 7b). Non-quantitative ROS measurement (Fig. 8) was also performed on the cells exposed to the nanomaterials and ionic copper, over a period of 4 hrs. Exposure to CuO spheres and rods caused considerably higher oxidative stress compared to spindles and ionic copper.

4. DISCUSSIONS

4.1 Effect of particle shape on colloidal stability and dissolution behaviour

This study shows how the particle shape can affect the stability and dissolution behaviour of particles with the same chemical composition i.e. CuO nanoparticles (i.e. spheres rods and spindles). Different shapes of the nanoparticles resulted in differences in their respective specific surface areas (SSA), with the highest SSA for the smallest CuO-s nanoparticles, followed by rods and CuO-spindles. The shape did have a considerable effect on ξ of the nanoparticles with spindles having the lowest ξ

followed by rods and spheres. On increasing the temperature (up to 50°C), the shape of the nanoparticles played a further role in the decrease of ξ, as shown in Fig. 4a. All the nanoparticles showed a decrease in ξ with increasing pH (up to their respective point of zero charge). The shape of the nanoparticles influenced the measured PZC, following the order of $PZC_{CuO\text{-}spindles} < PZC_{CuO\text{-}r} < PZC_{CuO\text{-}s}$. This order reflects the stability of suspensions at neutral pH, whereby the spheres are most stable being the farthest away from the PZC at this pH while spindles should be least stable as being closest to PZC. Differences in the PZC of the samples can be accredited to the different shapes altering the surface area and surface energy of the nanoparticles resulting in different adsorption and affinity of protons on the surface (Mills et al. 1993). Various intrinsic (particle size, crystal phase, synthesis method) and extrinsic parameters (ionic strength, presence of organic matter) can affect the PZC for samples (Suttiponparnit et al. 2011; Liao et al. 2009), and thus the stability of the nanoparticles. It is important to note that the differences in the shape of the nanoparticles also has a further effect on other aspects of the nanoparticles (such as, size, surface area, surface energy etc.), which would all in turn contribute to the differences observed in the physicochemical properties of the CuO nanoparticles in this study.

Dissolution experiments (Fig. 5) on nanoparticles dispersed in 1mM $NaNO_3$ indicate that particle shape had a significant effect on the amount of Cu dissolved over the 7 days period. For CuO-s and CuO-r nanoparticles, an apparent equilibrium Cu concentration (1 and 0.4 mg/L, respectively) was reached within 72 hrs from the start of the experiment and no significant change for the remaining duration of the experiment was observed. In comparison, for CuO-spindles the rate of dissolution

was slower (Fig. 5a-b). There was also significant difference in the quantity of Cu released over a 7 day period, with 2.5% dissolution reported for CuO-s and significantly lower 0.8% dissolution for CuO-spindles. The relative differences in the dissolution between the three types of CuO nanoparticles could be due to the shape related differences in their specific surface areas and their suspension stability, as reported for various other particles (Gunawan et al. 2011: Bian et al. 2011). To gain a further understanding of the effects of starting concentration on dissolution, dissolution of CuO-spindles, was measured over a 7 day period using a range of starting concentration inside the dialysis bag, as shown in Fig. 5c-d. The quantity of Cu released increased as the starting particle concentration increased. However, on normalising the data by mass the pattern is somewhat different. With increasing the particle concentration beyond 10 mg/L, a decrease in mass percentage of nanoparticles dissolved throughout the time period is observed. For example, after 6 days the percentage of CuO-spindles dissolved for 5, 10, 20, 50 and 750 mg/L starting concentration was 11%, 17%, 13%, 8% and 0.8%, respectively. This clearly shows that in a low exposure concentration scenario, a larger proportion of the nanoparticles will be dissolved and thus the contribution of particulate driven toxicity effect will be much lower than in high exposure concentration studies. This also has particularly important implications in laboratory experiments, where serial dilutions are tested. Such concentration dependent dissolution has been also reported for other nanoparticles (Liu and Hurt, 2010).

In contrast to tests performed in water, when particles were suspended in serum free cell culture media (DCCM-1), there was a significant increase in the dissolution of all three shapes of CuO nanoparticles, with >50% dissolution after 24 hrs

exposure, (Table 2). To check whether the presence of high concentration of inorganic salts in the cell culture media influenced the dissolution, CuO-s nanoparticles were suspended in US EPA approved freshwater and seawater (media containing high concentration of inorganic salts). The results indicated a much-reduced dissolution, most likely due to significant particle agglomeration in the media (Supporting Information S4). Similar results were also obtained by Gunawan et al (2011), wherein dissolution of 14 nm CuO nanoparticles was significantly reduced in high inorganic salt content media but enhanced (up to 95% dissolution) in bacterial culture media containing high amount of amino acids. The presence of various amino acids in the DCCM-1 medium could be the critical factor in enhancing dissolution. The presence of peptides has been shown to increase the dissolution of CuO nanoparticles (Midander et al. 2009), which may be explained by a well-known tendency of Cu to bind to amino acids and in particular to histidine, and glutamine (Neumann et al. 1967), both of which are present in the DCCM-1 media. In addition, the presence of citric acid has also been shown to catalyse the dissolution of copper oxide (Kwang Ko et al. 2010), due to the chelating action of citric acid. Therefore, the dissolution of CuO particles could also be expected to be higher in lysosomol fluid due to the high content of citric acid (Marques et al. 2011).

4.2 Effect of particle shape on biological response

Biological studies (Fig. 6-7) performed on transformed, human alveolar type-1 cells (TT-1 cells) showed that the presence of CuO-s and CuO-r nanoparticles were tolerated up to a concentration of 1 µg/mL, beyond which, there was a significant reduction in cell viability during 24 hrs exposure period. In contrast, there was no

significant reduction in cell viability on increasing CuO-spindle concentration, suggesting this particular CuO nanoparticles shape was not cytotoxic. In DCCM-1 media there was a significant dissolution for all three particle types; the highest for spheres and rods (>80%), followed by spindles (>60%) over the 24hrs exposure period. Since Cu ions have been shown to be cytotoxic (Blinova et al. 2010; Lei et al. 2008; Mortimer et al. 2010), it is possible that the high concentrations of dissolved Cu could have been a significant contributor to the observed cytotoxicity of the nanoparticles. However, data obtained in this study indicates that the cytotoxicity induced by ionic Cu (at concentrations equivalent to that of the Cu content of the concentrations used for nanoparticles exposure) is not directly comparable with the cytotoxicity caused by exposure to the CuO-r and CuO-s nanoparticles themselves. In addition, even though CuO-spindles, undergoes >50%dissolution in DCCM-1 media, it has a significantly lower cytotoxic response in TT-1 cells compared to spheres and rods. Therefore, in this case, dissolved species of Cu do not solely account for the observed cytotoxicity in response to CuO-r and CuO-s exposure. Recent (eco)toxicological studies (Baek et al. 2011; Karlsson et al. 2008; Midlander et al. 2009) show that the toxicity generated by the exposure of CuO nanoparticles is also accounted by the nanoparticles themselves and not exclusive to dissolved copper. This could be explained due to the sedimentation of the particles in the cell culture media providing a higher degree of interaction with the cells deposited at the bottom (Cho et al. 2011; Midlander et al. 2009).

Another mechanism by which CuO nanoparticles can exhibit toxicity is oxidative stress**.** The exposure of the nanoparticles to TT-1 cell lines for a period of 4 hours resulted in increased oxidative stress on the cells (Fig.8). Exposure to spherical and

rod shaped nanoparticles caused considerably higher oxidative stress in the tested cells compared with spindles. On the other hand, exposure to ionic copper did not result in any considerable oxidative stress to the cells. The fact that all these particles agglomerate in the DCCM media and sediment under static condition on cells, can also lead to an increase in the oxidative stress on the cells (Cho et al. 2011; Plascencia-Villa et al. 2012). As shown in Fig. 7a, there was a marked decrease in release of IL-6 from TT-1 cells on increasing the concentration of CuO-s and CuO-r nanoparticles. The presence of low concentration (up to 5 μg/mL) of spherical and rod shaped nanoparticles did not cause a significant reduction in cell viability but did show a significant increase in IL-6 release compared to the baseline over the exposure duration. The higher proportion of cell death at increased nanoparticulate concentration can explain the reduction in release of IL-6 from TT-1 cells for CuO-s and CuO-r exposure. Even though the CuO-spindles did not have a significant effect on the viability of the cells, there was a considerable increase in IL-6, suggesting a bioreactive response to the nanoparticles. Such a response could be due to the dissolved copper released by CuO-spindles (Fig. 5c-d), or the presence of the nanoparticles themselves, or a combination of both.

5. CONCLUSIONS

Extensive nano-toxicological studies using spherical nanoparticles have provided valuable insights on the effect of particle characteristics (size, surface chemistry) on biological response. However, for engineered nanoparticles there seems to be very limited information on the relevance of shape on reactivity and biological response. This study therefore brings into light the important and complex role shape can play

for CuO particles in their physicochemical behaviour and also in their biological response. Our study suggests that the shape of the particles has a significant effect on the suspension stability and dissolution. Spherical particles showed higher suspension stability and dissolution compared to the rod and spindle shaped particles. However, these differences were found to be diminished when particles were suspended in relevant biological media i.e. cell culture media where it was also found that dissolution behaviour of all particles was markedly changed resulting in almost complete particle dissolution in biological media. This suggests strongly that dissolved copper is a significant factor in the biological response of CuO nanoparticles. The results generated in this study imply, however, that toxicity/inflammatory response induced in TT-1 cells by the nanoparticles cannot be solely correlated to dissolve particle fraction, and it is also the nanoparticles themselves that are having cytotoxic effects. The work is expected to instigate a more holistic understanding of the source of toxicity from other nanomaterials beyond CuO involving a wider range of particle physicochemical properties.

ACKNOWDLEDGEMENT

The research leading to these results has received funding from the QNano Project (for the work of SKM and AD) http://www.qnano-ri.eu from the European Community Research Infrastructures under the FP7 Capacities Programme FP7/2007-2013 under grant agreement no 262163 and NanoReTox (for the work of SN and DB) from the European Community's Seventh Framework Programme (NanoRetox-FP7/2007-2013) under grant agreement no CP-FP 214478-2.

SUPPORTING INFORMATION

Dissolution of CuO nanoparticles as assessed using different methods (dialysis and centrifugal filtration), dissolution of CuO nanoparticles and micron particles in 1mM $NaNO_3$, and dissolution of CuO nanoparticles in artificial freshwater.

REFERENCES

Ahamed M, Siddiqui MA, Akhtar I, Ahmad I, Pant AB, Alhadlaq HA. 2010. Genotoxic potential of copper oxide nanoparticles in human lung epithelial cells. Biochem Biophys Res Comm 396:578-83.

Baek YK, An YJ. 2011. Microbial toxicity of metal oxide nanoparticles (CuO, NiO, ZnO, and Sb_2O_3) to Escherichia coli, Bacillus subtilis, and Streptococcus aureus. Sci Total Environ 409:1603-8.

Bian SW, Mudunkotuwa IA, Rupasinghe T, Grassian VH. 2011. Aggregation and sisolution of 4 nm ZnO nanoparticles in aqueous environments: Influence of pH, ionic strength and adsorption of humic acids. Langmuir 27:6059-68.

Blinova I, Ivask A, Heinlaan M, Mortimer M, Kahru A. 2010. Ecotoxicity of nanoparticles of CuO and ZnO in natural water. Environ Poll 158:41-7.

Cho EC, Zhang Q, Xia Y. 2011. The effect of sedimentation and diffusion on cellular uptake of gold nanoparticles. Nat Nanotechnol 6:385-91.

Costa P, Sousa Lobo JM. 2001. Modeling and comparison of dissolution profiles. Eur J Pharm Sci 13;123-33.

Fahmy B, Cormier SA. 2009. Copper oxide nanoparticles induce oxidative stress and cytotoxicity in airway epithelial cells. Toxicol In Vitro 23:1365-71.

Franklin NM, Rogers NJ, Apte SC, Batley GE, Gadd GE, Casey PS. 2007. Comparative toxicity of nanoparticulate ZnO, Bulk ZnO, and $ZnCl_2$ to a freshwater microalga (Pseudokirchneriella subcapitata): The importance of particle solubility. Environ Sci Technol 41:8484-90.

Gratton SE, Ropp PA, Pohlhaus PD, Luft JC, Madden VJ, Napier ME, et al. 2008. The effect of particle design on cellular internalization pathways Proc Natl Acd Sci 105: 11613-8.

Gunawan C, Teoh WY, Marquis CP, Amal R. 2011. Cytotoxic Origin of Copper(II) Oxide Nanoparticles: Comparative Studies with Micron-Sized Particles, Leachate, and Metal Salts. ACS Nano 5:7214-25.

Huang X, Teng X, Chen D, Tang F, He J. The effect of the shape of mesoporous silica nanoparticles on cellular uptake and cell function. Biomaterials 2010;31:438-48.

Karlsson HL, Gustafsson J, Cronholm P, Moller L. 2009. Size-dependent toxicity of metal oxide particles—A comparison between nano- and micrometer size. Toxicol Lett 188:112-8.

Karlsson HL, Cronholm P, Gustafsson J, Moller L. 2008. Copper oxide nanoparticles are highly toxic: a comparison between metal oxide nanoparticles and carbon nanotubes. Chem Res Toxicol 21:1726-32.

Kim TH, Kim M, Park HS, Gong MS, Kim HW. 2012. Size-dependent cellular toxicity of silver nanoparticles. J Biomed Mater Res A 100:1033-43.

Kwang Ko C, Lee WG. 2010. Effects of pH variation in aqueous solutions on dissolution of copper oxide. Surf Interface Anal 42:1128-30.

Lei R, Wu C, Yang B, Ma H, Shi C, Wang Q, et al. 2008. Integrated metabolomic analysis of the nano-sized copper particle-induced hepatotoxicity and nephrotoxicity in rats: A rapid in vivo screening method for nanotoxicity. Toxicol Appl Pharmacol 232:292-301.

Li Y, Zhang W, Niu J, Chen Y. 2012. Mechanism of photogenerated reactive oxygen species and correlation with the antibacterial properties of engineered metal-oxide nanoparticles. ACS Nano 6:5164-73.

Liao DL, Wu GS, Liao BQ. 2009. Zeta potential of shape-controlled TiO_2 nanoparticles with surfactants. Colloids Surf A Physicochem Eng Asp 348:270-5.

Liu J, Sonshine DA, Shervani S, Hurt RH. 2010. Controlled release of biologically active silver from nanosilver surfaces. ACS Nano 4;6903-13.

Liu J, Hurt RH. 2010. Ion release kinetics and particle persistence in aqueous nano silver colloids. Environ Sci Technol 44:2169-75.

Lundqvist M, Stigler J, Elia G, Lynch I, Cedervall T, Dawson KA. 2008. Nanoparticle size abd surface properties determine the protein corona with possible implications for biological impacts. Proc Nat Acad Sci 105:14265-70

Marques MRC, Loebenberg R, Almukainzi M. 2011. Simulated biological fluids with possible application in dissolution testing. Dissolution Technologies August: 15-28

Midander K, Cronholm P, Karlsson HL, Elihn K, Moller L, et al. 2009. Surface Characteristics, Copper Release, and Toxicity of Nano- and Micrometer-Sized Copper and Copper(II) Oxide Particles: A Cross-Disciplinary Study. Small 5:389-99.

Mills A, Morris S. 1993. Photomineralization of 4-chlorophenol sensitized by titanium ioxide: a study of the initial kinetics of carbon dioxide photogeneration. J Photochem Photobiol A 71:71-83.

Misra SK, Dybowska AD, Berhanu D, Croteau MN, Luoma SN, Boccaccini AR, et al. 2012. Isotopically modified nanoparticles for enhanced detection in bioaccumulation studies. Environ Sci Technol 46:1216-22.

Misra SK, Dybowska AD, Berhanu D, Luoma SN, Valsami-Jones E. 2012. The complexity of nanoparticles dissolution and its importance in nanotoxicological studies. Sci Total Env 438 :225-32.

Mortimer M, Kasemets K, Kahru A. 2010. Toxicity of ZnO and CuO nanoparticles to ciliated protozoa *Tetrahymena thermophila*. Toxicology 269:182-9.

Navarro E, Piccapietra F, Wagner B, Marconi F, Kaegi R, Odzak N, et al. 2008. Toxicity of silver nanoparticles to *Chlamydomonas reinhardtii*. Environ Sci Technol 42:8959-64.

Neumann PZ, Sass-Kortsak A. 1967. The state of copper in human serum: evidence for an amino acid-bound fraction. J Clin Invest 46:646-58.

Pal S, Tak YK, Song JM. 2007. Does the antibacterial activity of silver nanoparticles depend on the shape of the nanoparticle? A study of the gram-negative bacterium *Escherichia coli*. App Environ Microbiol 73:1712-20.

Park EJ, Yi J, Kim Y, Choi K, Park K. 2010. Silver nanoparticles induce cytotoxicity by a Trojan-horse type mechanism. Toxicol In Vitro 24:872-8

Petros RA, DeSimone JM. 2010. Strategies in the design of nanoparticles for therapeutic applications. Nat Rev Drug Disc 9:615-27.

Plascecia-Villa G, Starr CR, Armstrong LS, Ponce A, Jose-Yacaman M. 2012. Imaging interactions of metal oxide nanoparticles with macrophage cells by ultra-high resolution scanning electron microscopy techniques. Integr. Biol. 4:1358-66.

Stoehr LC, Gonzalez E, Stampfl A, Casals E, Duschl A, Puntes V, Oostingh GJ. 2011. Shape matters: effects of silver nanospheres and wires on human alveolar epithelial cells. Part Fibre Toxicol 8:36.

Studer AM, Limbach LK, Van Duc L, Krumeich F, Athanassiou EK, Gerber LC, et al. 2010. Nanoparticle cytotoxicity depends on intracellular solubility: Comparison of stabilized copper metal and degradable copper oxide nanoparticles. Toxicol Lett 197:169-74.

Suttiponparnit K, Jiang J, Sahu M, Suvachittanont S, Charinpanitkul T, Biswas P. 2011. Role of surface area, primary particle size, and crystal phase on titanium dioxide nanoparticle dispersion properties. Nanoscale Res Lett 6:27.

Venkataraman S, Hedrick JL, Ong ZY, Yang C, Ee PL, Hammond PT, et al. 2011. The effects of polymeric nanostructure shape on drug delivery. Adv Drug Deliv Rev 63:1228-46.

Yu KO, Grabinski CM, Schrand AM, Murdock RC, Wang W, Gu B, et al. 2009. Toxicity of amorphous silica nanoparticles in mouse keratinocytes. J Nanopart Res 11:15-24.

Zhu J, Li D, Chen H, Yang X, Lu L, Wang X. 2004. Highly dispersed CuO nanoparticles prepared by a novel quick precipitation method. Mater Lett 58:3324-27.

List of Tables and Figures

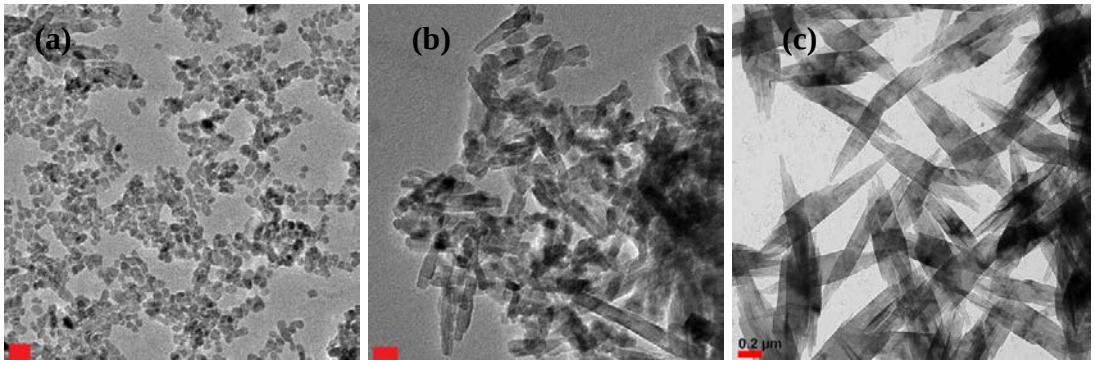

Figure 1 TEM images of (a) CuO-s (scale bar =20 nm), (b) CuO-r (scale bar =20 nm), and (c) CuO-spindles (scale bar =200 nm) nanomaterials

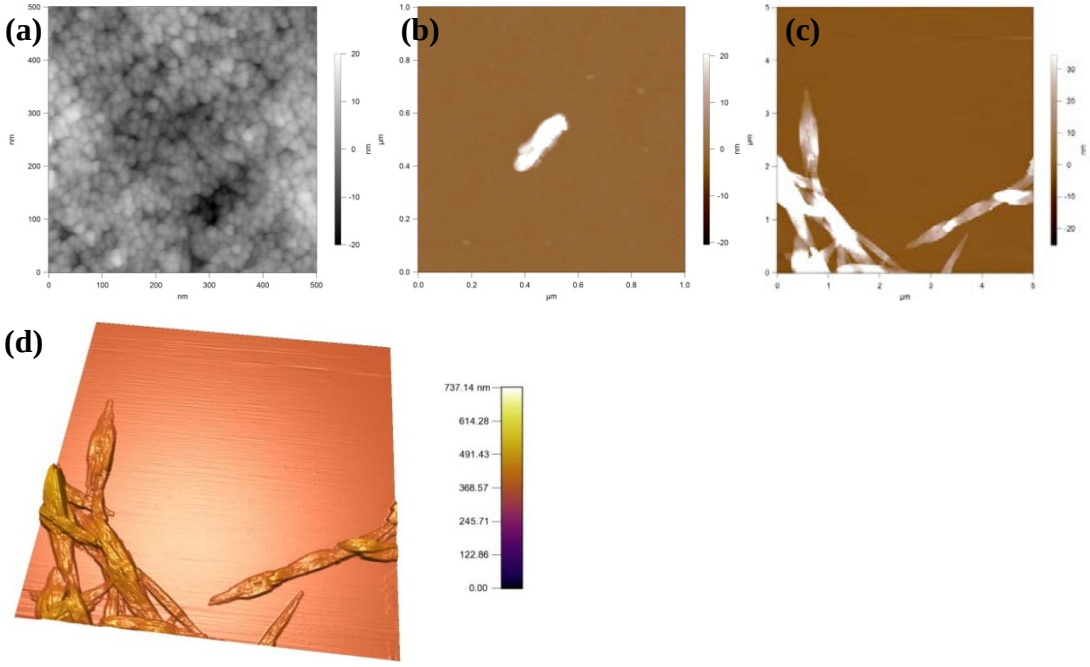

Figure 2 AFM images of (a) CuO-s, (b) CuO-r, and (c,d) CuO-spindles

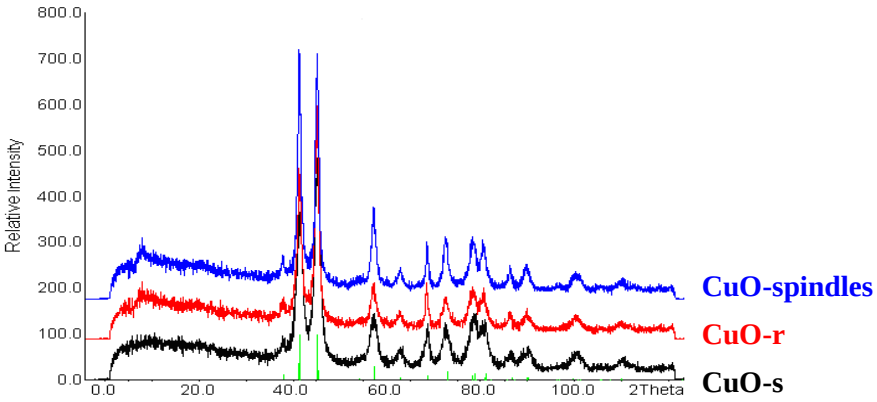

Figure 3 XRD pattern for the three different shapes of CuO nanoparticles particles indicating them to be of tenorite (green vertical markers) phase. The peaks have been shifted vertically for clarity.

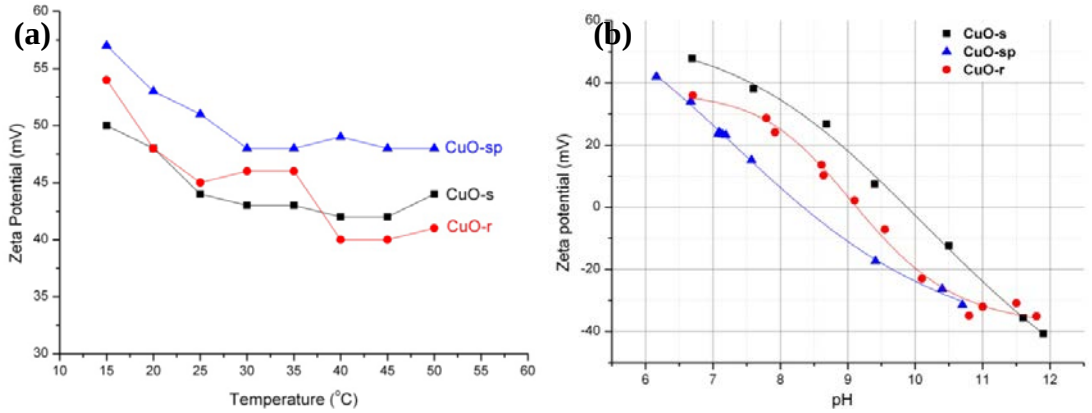

Figure 4 (a) Effect of temperature on zeta potential for three different shapes of CuO nanoparticles. (b) Effect of pH on zeta potential measurements indicating point of zero charge (PZC) for CuO-s, CuO-r and CuO-sp nanoparticles in 1 mM $NaNO_3$ media at room temperature.

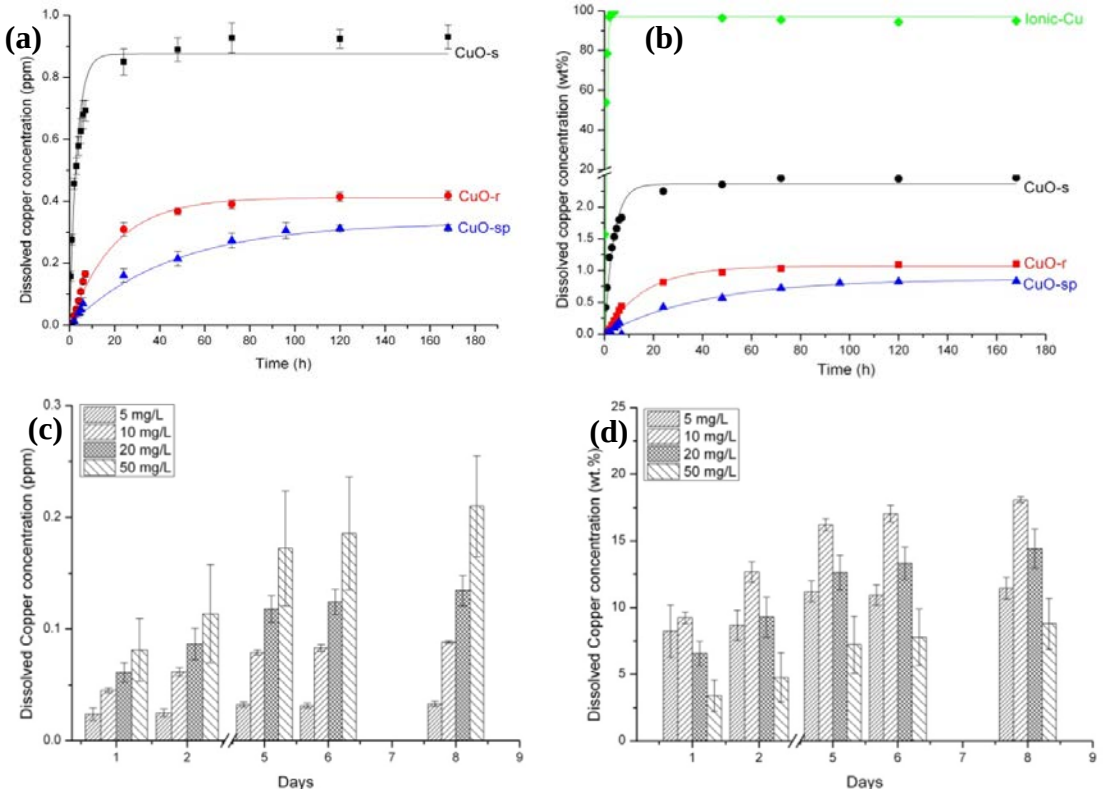

Figure 5 Dissolved Cu release from three different shapes of CuO nanoparticles and ionic copper source in 1 mM $NaNO_3$ at 25°C expressed in (a) dissolved copper in solution, (b) proportion to the original mass of CuO nanoparticles at the start of the experiment (mass %). For Figure (a) and (b) the starting Cu concentration inside the dialysis bag was kept constant at 750 mg/L and all data were fitted with a first order exponential growth equation described in Equation 1. (c) Dissolved Cu released from CuO-spindles using a range of starting concentrations from 5-50 mg/L (ppm) expressed in concentration and (d) in proportion to the original mass of CuO spindles (mass %).

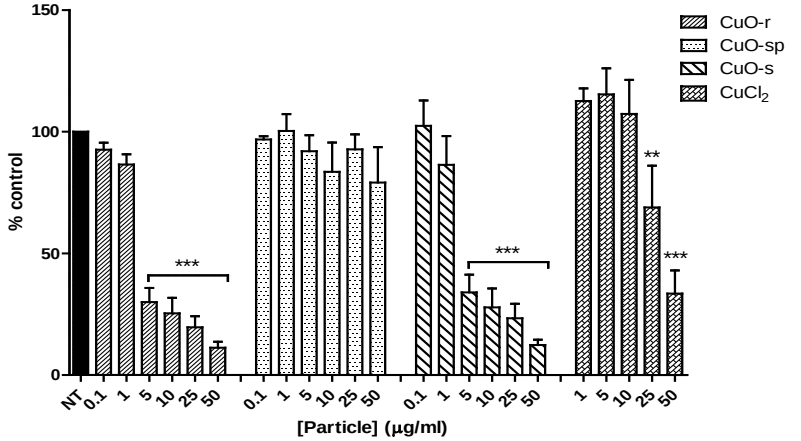

Figure 6 Effect of 24 hrs CuO nanoparticles exposure on TT-1 cell viability. TT-1 cells were serum starved for 24 hrs, then exposed to increasing concentrations of nanoparticles. Data are represented as percent viability (compared with non-treated (NT) control) and expressed as standard error of the mean for 4 individual experiments. Statistical significance was analysed by one-way ANOVA and compared with non-treated control (NT) ***p<0.001. The concentration expressed in µg/mL is for copper.

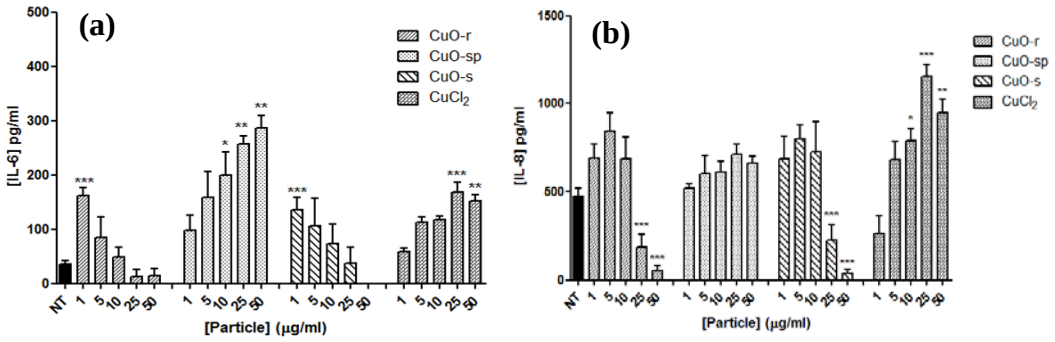

Figure 7 Effect of 24 hr CuO-r, CuO-spindles and CuO-s nanoparticles exposure on TT-1 cell showing (A) IL-6 (B), IL-8. TT-1 cells were serum starved for 24 hours, then exposed to increasing concentrations of nanoparticles. Cytokine release was measured by ELISA and data are expressed as concentration, extrapolated from standard curves. Data are expressed as standard error of the mean for 3 individual experiments. Statistical significance was analysed by one-way ANOVA and compared with non-treated control (NT) *p<0.05, **p<0.01, ***p<0.001. The concentration expressed in µg/mL is for copper.

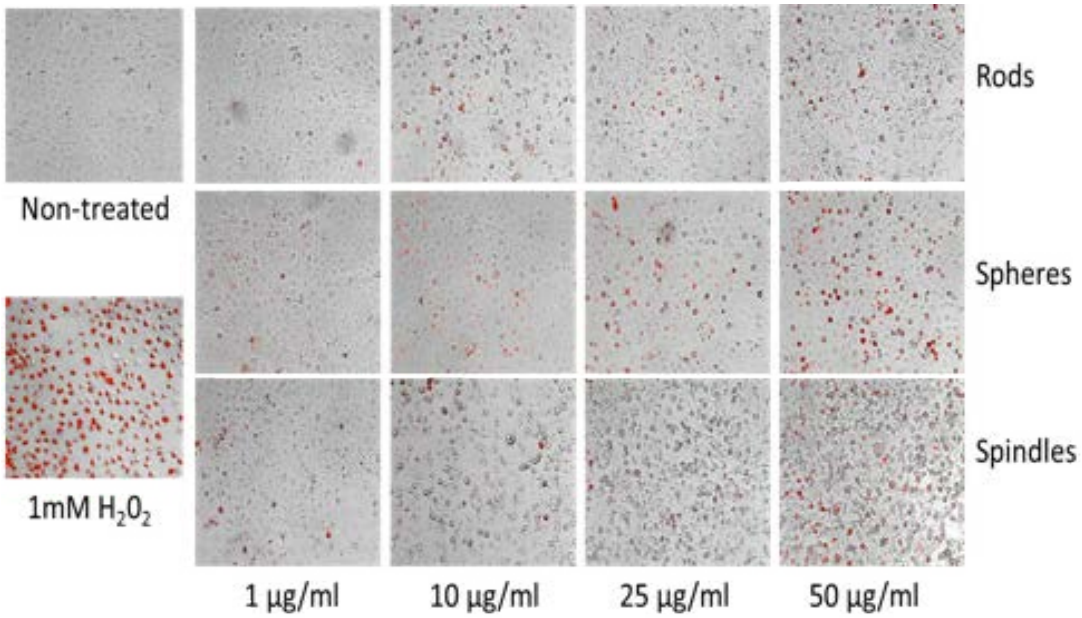

Figure 8 Effect of 4 hour CuO-r, CuO-spindles, and CuO-s nanoparticles exposure on reactive oxygen species generation in TT-1 cells. TT-1 cells were serum starved for 24 hours, then exposed to increasing concentrations of particles for 4 hours. After exposure, cells were washed 3 times and then incubated with dihydroethidium, which, upon oxidation by free radicals, intercalates with DNA and stains the cell nuclei red. Concentrations of particles are indicated on the figure and each image is taken at 10x magnification. Treatment with 1mM H_2O_2 provided a positive control.